

RSC Advances



This is an *Accepted Manuscript*, which has been through the Royal Society of Chemistry peer review process and has been accepted for publication.

Accepted Manuscripts are published online shortly after acceptance, before technical editing, formatting and proof reading. Using this free service, authors can make their results available to the community, in citable form, before we publish the edited article. This *Accepted Manuscript* will be replaced by the edited, formatted and paginated article as soon as this is available.

You can find more information about *Accepted Manuscripts* in the [Information for Authors](#).

Please note that technical editing may introduce minor changes to the text and/or graphics, which may alter content. The journal's standard [Terms & Conditions](#) and the [Ethical guidelines](#) still apply. In no event shall the Royal Society of Chemistry be held responsible for any errors or omissions in this *Accepted Manuscript* or any consequences arising from the use of any information it contains.

ARTICLE

Investigations of wettability of graphene on a micron-scale hole array substrate

Cite this: DOI: 10.1039/x0xx00000x

Received 00th January 2015,
Accepted 00th January 2015

DOI: 10.1039/x0xx00000x

www.rsc.org/

Yun Zhao^{a, b}, Gang Wang^b, Wenbin Huang^c, Xiaokun Fan^d, Ya Deng^b, Jian Zhang^b, Tongbo Wei^a, Ruifei Duan^{a, *}, Junxi Wang^a, Lianfeng Sun^{b, *}

In this work, graphene grown by chemical vapour deposition are transferred onto a micron-scale hole array (MSHA) substrate by a polymer-free transfer process. The graphene adheres to the walls of the microholes and comply with the morphologies of the micron-scale hole substrate. In contrast to previous reports of partial-transparency of wettability of graphene on a plane substrate, the wettability of graphene on the micro-scale hole array substrate is found to be hydrophobic with a contact angle of 93.1°. This is quite different from that of graphene on planar SiO₂/Si substrate, which is hydrophilic with a contact angle of 83.0°. We find that micron-scale hole array substrate has a regulation effect on wettability of graphene when the graphene almost completely comply with the morphology of the micron-scale hole array substrate surface and the change from hydrophilic to hydrophobic provides a guide for design surfaces with controllable wettability.

Introduction

Graphene, composed of a two-dimensional (2D) honeycomb lattice of carbon atoms¹, has attracted great interest due to its excellent physical and chemical properties. A decade after the isolation of graphene from the graphite,² the field of graphene has seen rapid processes in both understanding its fundamental properties and developing its potential for applications.

The wettability, which is one of the most important characteristics of a solid interface, has attracted considerable attention in many fields recently. It can reflect the changes of characteristics of a solid surface, including the chemical composition and the geometric microstructure. The wettability has a broad influence on the performances of applied devices for various fields, such as optoelectronics³, electric generator⁴, energy storage⁵, sensors and surface coating⁶.

Previous studies have demonstrated that the substrate on which graphene rests strongly influences the chemical reactions occurring on top of the graphene surface.^{7,8} The most commonly used substrate for graphene device is a 300 nm silicon dioxide (SiO₂) supported by a layer of doped silicon (Si). Therefore the wettability of graphene on SiO₂ is one of the most important parameters. The partial-transparency of

graphene can expound the wettability of graphene on plane substrate.^{9,10} By using molecular dynamics (MD) simulations Driskill et al. drew a similar conclusion.¹¹ However, the effect of graphene's surface morphology to wettability of graphene is still not clear. Bong et al. studied the wetting properties of graphene-laminated micropillar structures and they improved it by increasing the height of graphene-laminated micropillar structure.¹² Therefore, more surface studies are required to understand and control the water wettability of graphene.

In this article, we fabricate the graphene/SiO₂ micron-scale hole array (MSHA) substrate through direct (polymer-free) transferring graphene to SiO₂ MSHA substrate, and investigate the wettability of graphene on the SiO₂ micro-scale hole array substrate.

Experimental

The substrates used herein are SiO₂/Si substrates. The 300nm SiO₂ films were deposited onto doped Si substrates by plasma-enhanced chemical vapor deposition (PECVD) at about 300°C using nitrous oxide (N₂O) and silane (SiH₄) as gas precursors. By employing Nikon stepper lithography equipment (Nikon NSR 1755i7A), SiO₂ MSHA pattern can be obtained on the

plane SiO₂ substrate; Then inductively coupled plasma (ICP) etching of SiO₂ was carried out; the remaining photo resist was finally removed to obtain the SiO₂ MSHA substrate.

Graphene was synthesized by atmospheric pressure chemical vapor deposition using a copper foil (25- μm -thick, 99.8%, Alfa Aesar) as a catalyst. The Cu foil was ultrasonically cleaned in acetone. Then the oxide layer on Cu was removed by dilute hydrochloric acid. After the pre-cleaning process, the copper foil was annealed at 1030°C for 30 min under a 100-sccm (standard cubic centimeter per minute) hydrogen and 300-sccm argon atmosphere. The graphene was synthesized under 10-sccm methane and 100-sccm hydrogen and 300-sccm argon for 30min at 1030°C. During the cooling of the chamber down to room temperature, 100-sccm hydrogen and 300-sccm argon was kept to flow through the furnace.

After the synthesis, the graphene was transferred from the copper to a SiO₂/Si substrate as the following: Firstly, the graphene grown on the back side of the Cu foil is etched away by oxygen plasma treatment. After the treatment, the graphene on the front side of the Cu foil remain untouched. Then, the Cu foil is etched in 2M FeCl₃ for 2 hours and rinsed twice with deionized water. The graphene on the front side of Cu will come off and float on the surface of the solution. Finally, the graphene was transferred onto the SiO₂/Si substrate. All the samples were dried for two days in the nitrogen cabinet, and then the contact angle was immediately measured at room temperature and atmospheric condition.

It is well known that wettability is decided simultaneously by chemical composition and the geometrical microstructure of the surface.^{13,14} The contact angle (CA), which can be measured by an angle spanned at the intersection of the tangent line of liquid and the baseline of substrate on a macroscopic level, quantifies the average wettability of a solid surface by a liquid via the Young equation. We performed static contact angle measurements by placing a droplet of deionized water on the surface of the various substrates. Firstly, a 1 μL water droplet was generated using the automatic dispenser of the goniometer. The sessile droplet was formed by fixing the needle and approaching the substrate parallel to the needle direction with a very gentle feed rate of a few micrometers per minute. Then, image of drop was captured and the three-phase contact point was identified, which was the highly delicate process. The Young-Laplace theoretical model based on the axisymmetric-drop-shape analysis profile was selected and the tangent line of the goniometer was adjusted to the contact points to obtain the CA automatically.

The quality and layer number of graphene were characterized by high resolution transmission electron microscope (HRTEM, Tecnai F20) and Raman spectra. The Raman spectra of our samples with graphene films were collected using a 514nm laser which is excited from an argon ion laser. The contrasts of SiO₂ MSHA substrate with and without graphene were studied using an optical microscope (Leica DM4000), a scanning electron microscope (SEM, Hitachi S-4800) and an atomic force microscope (AFM, Veeco D3100). The SEM measurements were taken under high vacuum at an accelerating voltage of 10kV. AFM imaging was performed in tapping mode under ambient conditions. The average roughness can be calculated from the topographical images by atomic force microscopy. CAs were measured by the sessile-drop method with deionized water (1 μL) as probe liquids on a Dataphysics OCA20 CA system at room temperature.^{15,16} The average CA value was obtained by

measuring more than five different positions for the same sample.

Results and discussion

In order to confirm the graphene's layer number and investigate the microstructure of the samples, HRTEM characterization was used. The continuous graphene film was transferred onto a TEM grid by substrate etching. The edge of graphene tends to form folds, making it easier to distinguish from the surrounding grids and to count the number of layers. The HRTEM image in Figure 1a clearly shows the layered structure of the synthesized graphene. This indicates that the multilayer graphene have 4 or 5 graphene layers. To further characterize the graphene quality and count the number of graphene layers^{17,18}, Raman spectroscopy was performed. Typical Raman spectra of polymer-free graphene samples before and after direct transfer onto SiO₂ MSHA substrate are shown in Figure 1b. The three most intense Raman peaks are located at ~ 1356 , ~ 1581 and ~ 2719 cm⁻¹, representing D, G and 2D modes, respectively. The intensity ratio I(G)/I(2D) of graphene on copper is 1.86.¹⁹ The Raman spectra show relatively low intensity of D peak, indicating the presence of structural disorder, such as domain boundaries and structural defects. The similar intensities of D peak between pristine graphene and that after transferring indicate that the defects from transferring progress are negligible. Combining TEM with Raman characterizations, we can explicitly evaluate the number of graphene layers (4~5 layers) and the effective polymer-free graphene transfer progress.

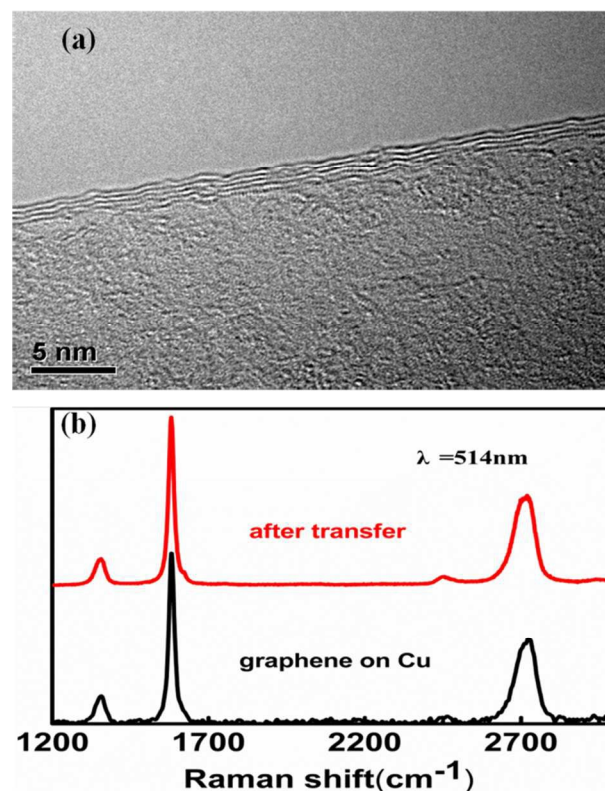


Figure 1. (a) Typical High Resolution Transmission Electron Microscopy (HRTEM) image of the graphene used in the experiment. The graphene is well graphitized and have four or five layer. (b) Typical Raman spectra of the graphene grown by chemical vapor deposition on copper

and that after the graphene is transferred onto micron-scale hole array (MSHA) SiO₂/Si using polymer-free transfer process.

For CVD-grown graphene, it is important to transfer them to other substrates for research and applications. In previous reports⁷⁻⁹, the polymer-assisted transfer methods are commonly used for transferring graphene to other substrate. For wettability studies of graphene, polymer residues cannot be neglected because surface contamination of graphene will have a very effect on the results²⁰. This means the cleanliness of graphene is extremely important when studying its wettability. Polymer-free graphene transfer process enables direct CVD-grown graphene to be transferred to the substrates. Extra processes to remove polymer residues and concerns about graphene surface contaminations are not needed.^{21,22} We directly transfer polymer-free graphene to target substrates minimizing contamination and preventing obscuring their intrinsic water wettability.

To examine the alignment and morphology of the substrates and the SiO₂ MSHA substrates covered with graphene, SEM examinations were performed. Figure 2a shows the pattern of SiO₂ MSHA substrate. It can be seen that the diameter of hole is about 1.3μm and the period is 2.0μm. The holes are clear and the edges of hole are smooth. Figure 2b, 2c and 2d show the SEM images of SiO₂ MSHA substrates covered with 4-5 layers graphene. It can be seen that the surface of graphene is highly continuous and no obvious wrinkled and folded regions are observed in large scale (Fig. 2b), indicating the high quality of the graphene/SiO₂ MSHA substrate. Wrinkles are a very common phenomenon probably forming to relieve thermal stress during the cooling, and they often collapse when the copper substrate is etched away and the graphene is transferred to target substrates (Fig. 2c and Fig. 2d).²³⁻²⁵ Compared with the conventional polymer transfer process, the direct transfer process is much cleaner than the standard polymer transfer process as it involves fewer potential contaminants on the surface such as polymer and acetone, which have great influence on wettability of graphene. Due to the surface tension, the suspended graphene regions near the edges of the holes will likely be broken and torn during and the drying process in the nitrogen cabinet (arrow B in Figure 2c).

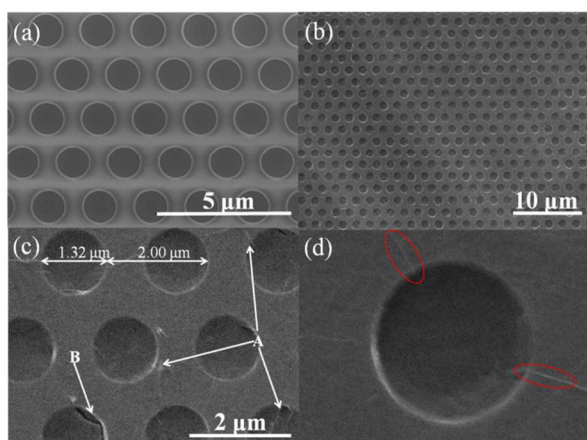


Figure 2. (a) Typical SEM image of micron-scale hole array (MSHA) SiO₂/Si. It shows that the holes are regular and uniform. The diameter of hole is about 1.3μm and the period is 2.0μm. (b) SEM image of graphene adsorbed on MSHA SiO₂/Si. It can be seen that the surface of graphene is clean and continuous. (c) Higher magnification SEM image of the graphene on MSHA SiO₂/Si. There are some

wrinkles (as indicated by arrow A) and few cracks (as indicated by arrow B). (d) Higher magnification SEM image of an individual hole covered with graphene. The graphene is continuous and some wrinkles can be found as shown by the circles.

The above SEM images indicate that this polymer-free transferring of graphene can result in complete substrate coverage, a strong coupling between the substrate and the graphene and a very clean graphene surface. Therefore, the graphene on SiO₂ MSHA substrate are well suited for contact angle test. In theory, description of contact angle has fertile information of sample's surface, but in reality many factors can complicate the situation. Except the continuity and cleanliness, the status of graphene on hole is an important factor to contact angle. In order to know whether or not the graphene is suspended across the holes, the height profiles of SiO₂ MSHA substrate with and without graphene are shown in Figure 3b. Along the dashed line in Figure 3a, the height profile of micron-scale hole substrate surface with 4-5 layers graphene is investigated by red curve, and the black curve is the height profile of pristine SiO₂ MSHA substrate without graphene. The depth of holes is ~130nm and the graphene almost completely complies with the morphology of the MSHA substrate surface to maximize surface adhesion. There is a balance relationship between the adhesion energy and elastic energy, which relates to what degree the features of the micron-scale hole substrate surface are faithfully followed. Obviously, the graphene will not touch the bottom of hole when the depth-to-width ratio is big enough. In short, the graphene structure studied here was an integral part of larger three-dimensional structures, embedded in a micron-scale hole matrix.

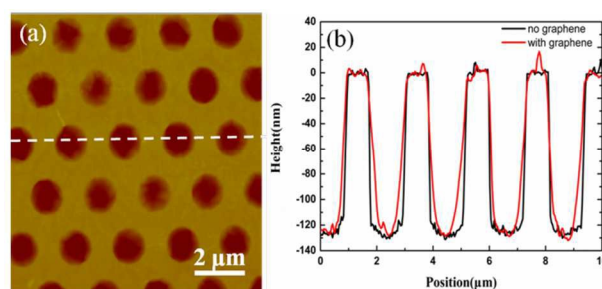


Figure 3. (a) Typical AFM image of graphene/MSHA SiO₂/Si. The AFM image is obtained in the tapping mode. (b) The height profiles of MSHA SiO₂/Si (black curve) and graphene/MSHA SiO₂/Si (red curve, along the dashed line in (a)). The similar depths of two curves indicate that the graphene is adsorbed onto the bottom of each individual hole.

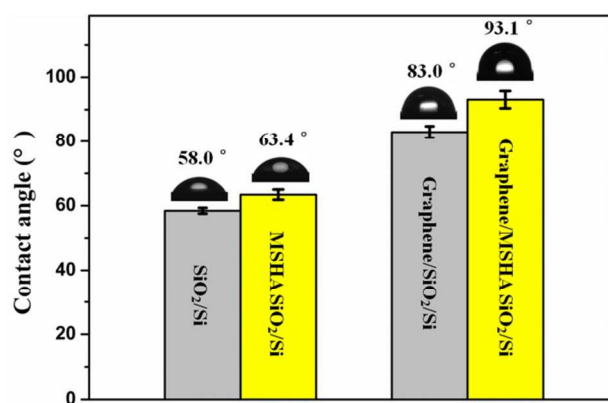


Figure 4. The water contact angles on different kinds of substrate. The water contact angle on SiO₂/Si and micron-scale holes array (MSHA) SiO₂/Si substrates are 58.0 and 63.4 degree, respectively. After the graphene is transferred onto the two kinds of substrates, the contact angles increase to 83.0 and 93.1 degree, respectively. The change from hydrophobic to hydrophilic provides a guide for design surfaces with controllable wettability.

As can be seen from Figure 4, the water CA on plane SiO₂ is ~58.0°. After microscale holes array are made on plane SiO₂ (SiO₂ MSHA substrate), the water CA becomes 63.4°. When the graphene was transferred onto the plane SiO₂, the water CA increases to ~83.0°, which is similar to that reported in Ref. 10 by Shih *et al.*. After the SiO₂ MSHA substrate was covered with the graphene, the water CA becomes ~93.1°. This value of contact angle is near the highest attainable angle of 96° on a graphene coated surface by Shih's theoretical predictions¹⁰. The increase of water contact angle by the graphene on plane SiO₂ substrate is 25° (83.0°-58.0°). For SiO₂ MSHA substrate, the increase of water contact angle by the graphene is 29.7° (93.1°-63.4°). This suggests that the wettability of graphene is partial-transparent and the increase in contact angle is from the SiO₂ MSHA substrate. That is to say SiO₂ MSHA substrate has a regulation effect on wettability of graphene when the graphene almost completely comply with the morphology of the MSHA substrate surface. And this change from hydrophobic to hydrophilic provides a guide for design surfaces with controllable wettability.

When a water droplet on a surface of solid substrate, the surface roughness factor should be consider during the evaluation of the surface wettability. There are two equations (Wenzel and Cassie equations), which are commonly used to correlate the surface roughness with the apparent CA of a liquid droplet on a solid substrate. In the Wenzel case, the apparent water CA θ_w will be described by Wenzel equation:

$$\cos \theta_w = r \cos \theta \quad (1)$$

where r is the surface roughness (>1), θ is the water contact angle in plane surface. From Wenzel equation, we can conclude that: if $\theta < 90^\circ$, then $\theta_w < \theta$. This means that after digging holes array on plane substrate, the water CA will be decreased. In our experiment, the water CAs on the MSHA substrate with and without graphene are larger than that on the plane substrate, respectively. These experimental data show that the states of water droplet on the micro-scale holes array substrate with and without graphene are not in agreement with the Wenzel case.

In Cassie case, the relationship between the contact angle

of the flat substrate θ and that of micron-scale hole substrate θ_r is expressed by Cassie and Baxter equation:

$$\cos \theta_r = r f_1 \cos \theta - f_2 \quad (2)$$

where r is the roughness factor, which is defined as the ratio of the actual surface area of a rough surface to the projected area, and the value is 1.16, f_1 and f_2 are the fractional interface areas of graphene surface and air in the holes, respectively. We can roughly estimate f_1 and f_2 from known contact angles. The contact angle θ for water on the flat SiO₂ substrate covered with graphene is $83.0 \pm 1.8^\circ$ and the contact angle θ_r for water on graphene covered micron-scale hole substrate is $93.1 \pm 2.7^\circ$. By using these values, f_1 and f_2 are calculated to be 0.83 and 0.17, respectively. In contrast, the contact angle θ for water on the flat SiO₂ substrate is $58.0 \pm 0.9^\circ$ and the contact angle θ_r for water on micron-scale hole SiO₂ substrate is $63.4 \pm 1.6^\circ$, and f_1 and f_2 are calculated to be 0.89 and 0.11. Therefore, these data are in agreement with the results of the Cassie case. That is to say, the states of water droplet on the SiO₂ micro-scale holes array substrate with and without graphene are both in the Cassie case. These results, almost consistent values of f_1 and f_2 , further confirm that the MSHA substrates with and without graphene have similar regulation effect. It is easy to deduce from this equation that increasing the value of f_2 will lead to the increase of θ_r . Accordingly, the more percentage of hole area on MSHA substrates with graphene can lead to the higher CA of water.

The dynamic wetting process of a water droplet on a hole-arrayed hydrophilic surface can theoretically be predicted using molecular dynamics simulations. Similarly, the holes accelerated the slow flow, while also resisting or pinning the fast flow, as the results published by Yuan & Zhao²⁶. They obtained the scaling laws for two regimes, $R \sim t^{1/3}$ for the rough surface and $R \sim t^{1/7}$ for the smooth surface (R is droplet radius). With the increase of roughness r , the propagation of the droplet increases.

Conclusions

In summary, graphene grown by chemical vapor deposition are transferred onto MSHA substrate by a polymer-free transfer process. The graphene adhere to the walls of the microholes and comply with the morphologies of the MSHA substrate. The wettability of graphene on the MSHA substrate is found to be hydrophobic with a contact angle of 93.1°. This is quite different from that of graphene on planar SiO₂/Si substrate⁷⁻¹⁰, which is hydrophilic with contact angle about 83.0°. This suggests that MSHA substrate has a regulation effect on wettability of graphene and the more percentage of hole area will lead to the increase of CA. We believe that the effect of graphene's surface morphology to wettability of graphene will be greatly facilitated by the regulation effect of MSHA and the change from hydrophobic to hydrophilic will provide a guide for design surfaces with controllable wettability.

Acknowledgements

This work was supported by National Science Foundation of China (Grant Nos. 10774032, 90921001), Instrument Developing Project of the Chinese Academy of Sciences (Grant No. Y2010031). This work was supported by the National Basic Research Program of China under Grant 2011CB301904, by the National High Technology Program of China under Grant 2011AA03A103 and 2011AA03A105.

Notes and references

^a Semiconductor Lighting Technology Research and Development Center, Institute of Semiconductors, Chinese Academy of Sciences, Beijing 100083, China.

^b National Center for Nanoscience and Technology, Chinese Academy of Sciences, Beijing 100190, People's Republic of China.

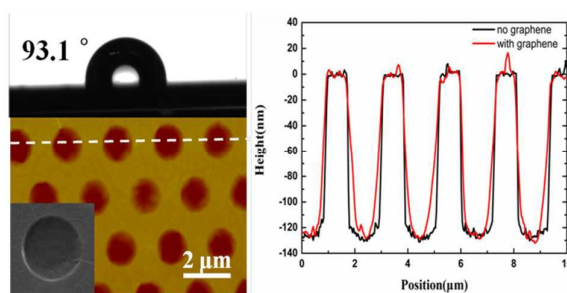
^c Institute of Nanotechnology and Microsystems, Mechanical Engineering College, Shijiazhuang 050003, China

^d School of Mechanical Electronic & Information Engineering, China University of Mining & Technology (Beijing), Beijing 100083, China.

* E-mail address: duanrf@semi.ac.cn and slf@nanoctr.cn

1. A. K. Geim, and K. S. Novoselov, *Nat. Mater.*, 2007, **6**, 183-191.
2. K. S. Novoselov, A. K. Geim, S. V. Morozov, D. Jiang, Y. Zhang, S. V. Dubonos, I. V. Grigorieva and A. A. Firsov, *Science*, 2004, **306**, 666-669.
3. J. Kim, C. Bayram, H. Park, C. W. Cheng, C. Dimitrakopoulos, J. A. Ott, K. B. Reuter, S. W. Bedell and D. K. Sadana, *Nat. Commun.*, 2014, **5**, 4836.
4. W. B. Huang, Y. Zhao, G. L. Wang, Z. T. Qiao, F. Q. Gao, X. W. Wang, G. Wang, Y. Deng, X. K. Fan, J. Zhang, R. F. Duan, X. H. Qiu and L. F. Sun, *RSC Adv.*, 2015, **5**, 34065-34069.
5. D. Wang, R. Kou, D. Choi, Z. Yang, Z. Nie, J. Li, L. V. Saraf, D. Hu, J. Zhang, G. L. Graff, J. Liu, M. A. Pope and I. A. Aksay, *ACS Nano*, 2010, **4**, 1587-1595.
6. M. Topsakal, H. Sahin and S. Ciraci, *Phys. Rev. B*, 2012, **85**, 155445-155451.
7. A. Chakradhar, N. Sivapragasam, M. T. Nayakasinghe, U. Burghaus, *Chem. Commun.*, 2015, **51**, 11463-11466.
8. Q. Wang, B. Bai, Y. Li, Y. Jiang, L. Ma, N. Ren, *RSC Adv.*, 2015, **5**, 10058-10064.
9. Z. Li, Y. Wang, A. Kozbial, G. Shenoy, F. Zhou, R. McGinley, P. Ireland, B. Morganstein, A. Kunkel, S. P. Surwade, L. Li and H. Liu, *Nat. Mater.*, 2013, **12**, 925-931.
10. C. J. Shih, Q. H. Wang, S. Lin, K. C. Park, Z. Jin, M. S. Strano and D. Blankschtein, *Phys. Rev. Lett.*, 2012, **109**, 176101.
11. J. Driskill, D. Vanzo, D. Bratko, A. Luzar, *J. Chem. Phys.* 2014, **141**, 18C517.
12. J. Bong, K. Seo, J. H. Park, J. R. Ahn, S. Ju, *J. Appl. Phys.*, 2014, **116**, 234303.
13. H. Li, X. Wang, Y. Song, Y. Liu, Q. Li, L. Jiang and D. Zhu, *Angew. Chem. Int. Ed.*, 2001, **40**, 1793-1796.
14. X. J. Feng and L. Jiang, *Adv. Mater.*, 2006, **18**, 3063-3078.
15. W. B. Huang, G. L. Wang, F. Q. Gao, Z. T. Qiao, G. Wang, M. J. Chen, L. Tao, Y. Deng, L. F. Sun, *Chin. Phys. B*, 2014, **23**, 046802.
16. X. Fan, L. Tao, Y. Deng, G. Wang, J. Zhang, Y. Zhao, W. Huang, H. Zhao, L. Sun, *RSC Adv.*, 2014, **4**, 59486-59490.
17. H. Q. Zhou, C. Y. Qiu, Z. Liu, H. C. Yang, L. J. Hu, J. Liu, H. F. Yang, C. Z. Gu and L. F. Sun, *J. Am. Chem. Soc.*, 2010, **132**, 944-946.
18. A. C. Ferrari, J. C. Meyer, V. Scardaci, C. Casiraghi, M. Lazzeri, F. Mauri, S. Piscanec, D. Jiang, K. S. Novoselov, S. Roth and A. K. Geim, *Phys. Rev. Lett.*, 2006, **97**, 187401.
19. I. Calizo, I. Bejenari, M. Rahman, G. X. Liu and A. A. Balandin, *J. Appl. Phys.*, 2009, **106**, 043509.
20. M. Jin, X. Feng, J. Xi, J. Zhai, K. Cho, L. Feng and L. Jiang, *Macromol. Rapid Comm.*, 2005, **26**, 1805-1809.
21. W. Regan, N. Alem, B. n. Alemán, B. Geng, C. a. I. Girit, L. Maserati, F. Wang, M. Crommie and A. Zettl, *Appl. Phys. Lett.*, 2010, **96**, 113102.
22. L. G. P. Martins, Y. Song, T. Zeng, M. S. Dresselhaus, J. Kong, and P. T. Araujo, *PNAS*, 2013, **110**, 17762-17761.
23. K. Kim, Z. Lee, B. D. Malone, K. T. Chan, B. Aleman, W. Regan, W. Regan, W. Gannett, M. F. Crommie, M. L. Cohen, A. Zettl, *Phys. Rev. B*, 2011, **83**, 245433.
24. W. L. Wang, S. Bhandari, W. Yi, D. C. Bell, R. Westervelt, E. Kaxiras, *Nano lett.*, 2012, **12**, 2278-2282.
25. A. Fasolino, J. H. Los, M. I. Katsnelson, *Nat. Mater.*, 2007, **6**, 858-861.
26. Q. Z. Yuan, Y. P. Zhao, *J. Fluid Mech.*, 2013, **716**, 171-188.

A table of contents entry



When graphene almost completely complies with the morphology of the SiO₂ micron-scale hole array (MSHA) substrate surface, the effect of graphene's surface morphology to wettability of graphene will be greatly facilitated by the regulation effect of MSHA.